nature geoscience
SUPPLEMENTARY INFORMATION
DOI: 10.1038/NGEO1422

Supplementary Information: Murray, Leinen, and Knowlton; "Links between iron input and opal deposition in the Pleistocene equatorial Pacific Ocean".

General Points

The numbered references in this Supplementary Information are provided at the end of this section, not with the references listed in the main article.

The lengthy Supplementary Table 2, which includes the opal and TOC data, can be found at the end of this Supplementary Information, after the "Supplementary References".

Water Column Processes Recorded in Sediment

Equatorial divergence in the equatorial Pacific Ocean leads to upwelling of cold, nutrient-rich waters from several hundred meters water depth[1]. This upwelling generates steep meridional gradients in primary productivity, diatom-associated chlorophyll, export flux, and phytodetritus laying on the seafloor[2,3] (Supplementary Fig. 1). These steep gradients within a few degrees of the Equator are characteristic of the region, are unrelated to changes in the concentration of any biogenic component[3,4], and are reflected in the meridional gradients of proxies of export production and sedimentary accumulation (Supplementary Fig. 1). Thus, the seafloor sediments record the patterns of biogeochemical processes operating in the uppermost waters.

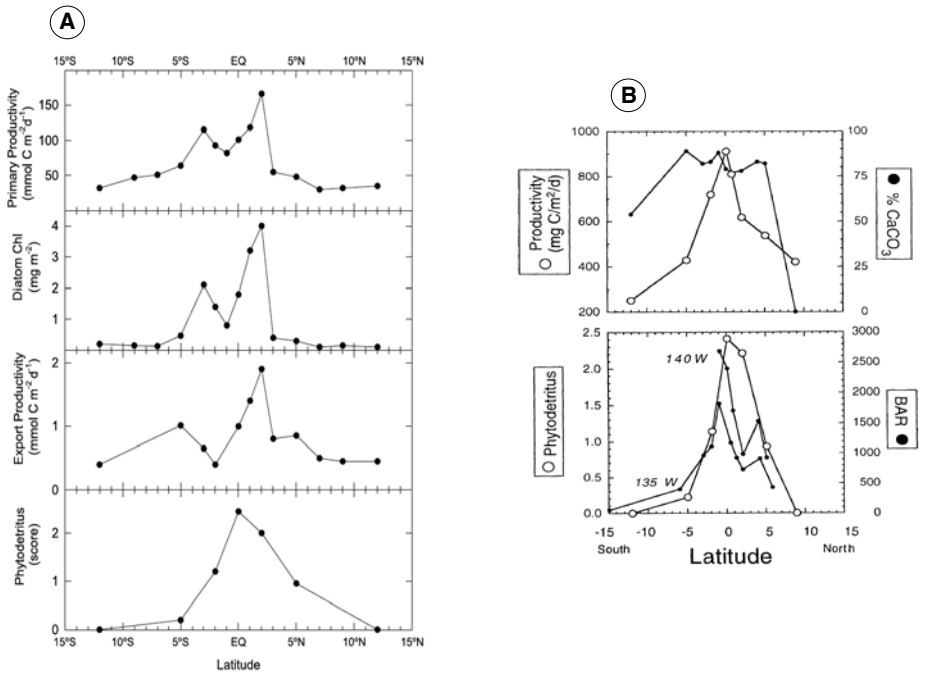

Supplementary Figure 1. Variation in water column and seafloor parameters across the 140W Joint Ocean Global Flux Study (JGOFS) meridional transect. From ref. 2-4 and sources therein.

Determination of Sedimentary Accumulation Rates: $\delta^{18}O$- and ^{230}Th-based Approaches

The bulk accumulation rate (BAR) of sediment is determined by the product of dry bulk density (DBD, mg/cm^3) and linear sedimentation rate (LSR, cm/kyr). The resulting BAR (in $mg/cm^2/kyr$) is not compromised by dilution or statistical closure, and allows for meaningful comparisons of rates of sedimentation processes.

As described in the main text, there is a major on-going debate in the literature about how best to determine the LSR term in the BAR calculation. Before presenting the similarities and differences between the $\delta^{18}O$-based[4] and ^{230}Th-based results[5,6] specifically in core PC72, it is worthwhile to note several matters relevant to the overall discussion.

First, both methods use the same $\delta^{18}O$-based stratigraphy[4] to determine the *age* of samples taken at given depths in the core. Thus, as we apply the two methods to core PC72, both use the same $\delta^{18}O$-based ages[4] and the same concentrations of $CaCO_3$ (ref. 4), opal (Supplementary Table 2), TOC (Supplementary Table 2), Fe (ref. 7), Ti (ref. 4), and Ba (ref. 4). The critical difference, however, is that the $\delta^{18}O$-based sedimentation rate interpolates between tie points for each sample to calculate the LSR. In contrast, the ^{230}Th approach uses the $\delta^{18}O$-determined age only in order to time-correct for U-series decay, and calculates the "instantaneous sedimentation rate" based on the amount of unsupported ^{230}Th. Thus, for both the ^{230}Th-based and $\delta^{18}O$-based sedimentation rates, the ages assigned to any given sample are based on the same $\delta^{18}O$-stratigraphic age[4].

Second, each method has its own intrinsic limitations. While this paper is not focused on the discussion of the evidence supporting each approach, it is important to consider briefly their uncertainties. The $\delta^{18}O$-based approach is fundamentally limited by the assumption of "linear", or constant, sedimentation between age-controlled tie points. While statistical techniques have been developed to accommodate this assumption, its validity probably varies with the resolution of age-control. While use of the ^{230}Th approach is increasing in recent literature (in part because an analogous approach is used to determine particle flux in the modern ocean and facilitates comparison between modern and paleoceanographic processes), this method also has uncertainties about its application. These include potential particle size fractionations, variable composition, effects of grain size, adsorption/dissolution, and other factors[8-11]. These issues, and others, remain the subject of ongoing study and debate that is likely to continue.

As noted, we do not preferentially endorse the application of either approach. We show below, consistent with the central thesis of the main text, that the Fe-opal relationship is more important than any other Fe-biogenic relationship, regardless of the sedimentation rate technique. Because the $\delta^{18}O$-based approach is emphasized in the main text due to its length and resolution, in this Supplementary Discussion we show the results of applying the ^{230}Th-based technique to our Fe and opal data.

The ^{230}Th measurements for accumulation rates in Core PC72 (ref. 5, 6) were made at different depths than our samples, so we interpolated the ^{230}Th-based

accumulation rates onto the depths of our samples. Bulk accumulation rates ($mg/cm^2/kyr$) from the two methods are plotted against their common $\delta^{18}O$-assigned age (Supplementary Fig. 2), and compared directly to each other (Supplementary Fig. 3). For the period of time from 0 to 38 kyr, the ^{230}Th-based accumulation rates[5,6] used ^{14}C-based ages, rather than $\delta^{18}O$-assigned ages (Supplementary Fig. 2). Thus, it is not appropriate to compare sedimentation younger than 38 kyr, and our discussion is only based on sediment older than 38 kyr.

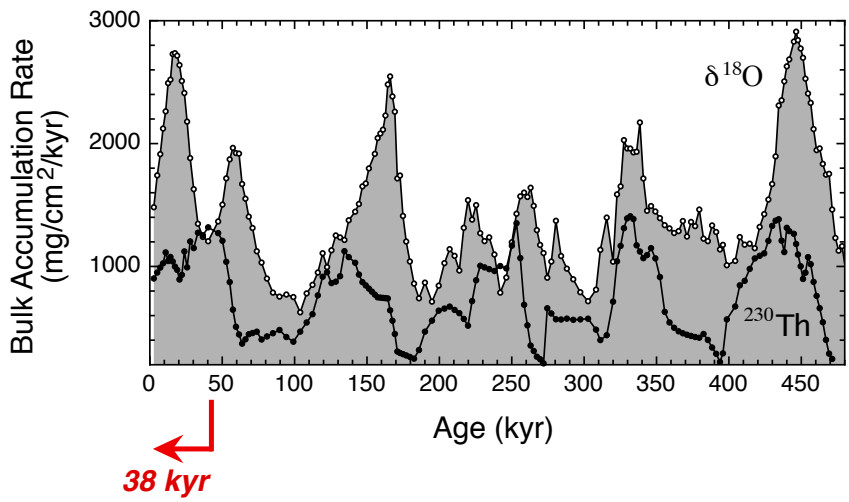

Supplementary Figure 2. Bulk accumulation rate, as determined by $\delta^{18}O$-based stratigraphy[4] (gray shaded) and ^{230}Th-based sedimentation rates (black dots), for Core PC72. For samples younger than 38 kyr, ages for the ^{230}Th-based samples were determined by ^{14}C (ref. 5,6).

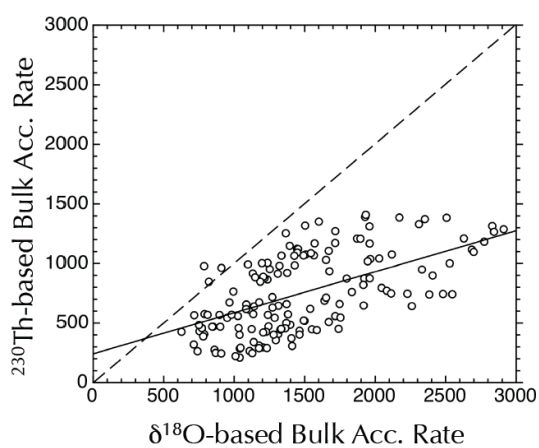

Supplementary Figure 3. Bulk accumulation rate ($mg/cm^2/kyr$) determined by $\delta^{18}O$-based stratigraphy[4] compared to bulk accumulation rate ($mg/cm^2/kyr$) determined by ^{230}Th-based sedimentation rates[5,6], for Core PC72. Data from younger than 38 kyr not included (see text). Dashed line is 1:1. Regression line (solid line): $^{230}Th = 0.344\ \delta^{18}O + 242$; $r = 0.59$ ($p < 0.001$).

The ^{230}Th-based method indicates lower bulk accumulation rates (Supplementary Fig. 3). There is general agreement that there are five periods of high sediment accumulation in the record (Supplementary Fig. 2), but the peaks are offset. The two approaches agree more strongly in timing of peak accumulation in sediment older than ~200-250 kyr. While some of the differences in timing and overall accumulation rate between the two approaches are significant, both suggest that bulk accumulation rate responded to a forcing with a period of approximately 100 kyr, well known in the equatorial Pacific[4-7]. Thus, these approaches are not responding to completely different sedimentation processes; the similarities between the profiles are too strong to reflect a totally disparate forcing. Similarly, comparing the ^{230}Th-normalized flux of ^{232}Th, which is inferred to document dust flux[5], to the δ^{18}O-based accumulation of total Fe (Supplementary Figure 4), also shows both similarities and contrasts. Notwithstanding the fundamental differences between ^{232}Th and Fe, let alone the respective uncertainties propagated through the calculations of the different bulk accumulation rates shown in Supplementary Figure 2, both curves show maxima through (approximately) 20-30 kyr, 65-75 kyr, 190-200 kyr, 220-230 kyr, and 270-280 kyr, as well as other smaller peaks and valleys. There are critical differences, as well, notably in the record older than ~300 kyr and in the duration of some of the peaks and valleys (e.g., in ^{232}Th centered at ~150 kyr).

To summarize, the differences identified in Supplementary Figs. 2, 3 and 4 are indeed important, and we certainly are not arguing that the techniques are interchangeable. We feel that our approach of comparing the Fe-opal relationship using *both* the δ^{18}O-based approach and the ^{230}Th-based approach is legitimate, as long as we compare accumulation rates internal to each system, and do not compare a δ^{18}O-based result to a ^{230}Th-based result.

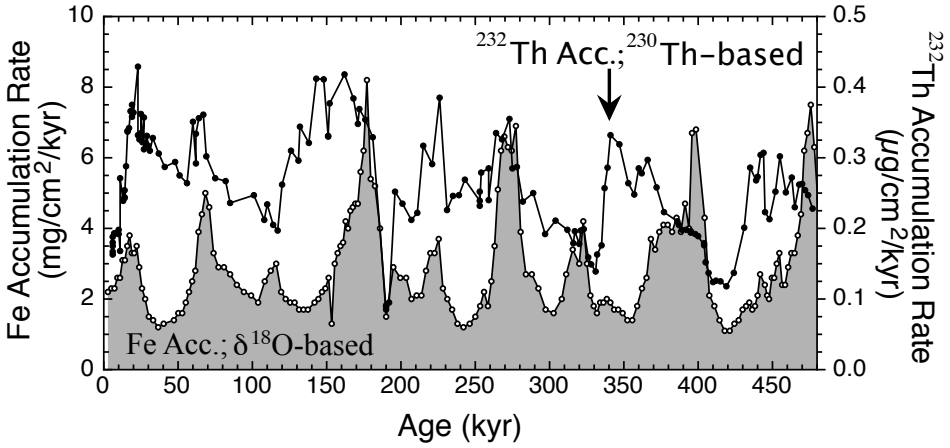

Supplementary Figure 4. Fe accumulation rate, as determined by δ^{18}O-based stratigraphy[4] (gray shaded) and the ^{230}Th-based accumulation of ^{232}Th (black dots, a proxy of dust flux[5]), for Core PC72. For samples younger than 38 kyr, ages for the ^{230}Th-based samples were determined by ^{14}C (ref. 5,6).

Our approach is confirmed by the time series of the accumulation of the sedimentary components calculated with the ^{230}Th-based rates (Supplementary Fig. 5), the direct x-y comparisons of the ^{230}Th-based rates (Supplementary Fig. 6, next page), and the Pearson correlation coefficients and p values for both the δ^{18}O- and ^{230}Th-based methods (Supplementary Table 1, next page). As with the concentration data, and with the δ^{18}O-based accumulation patterns, the ^{230}Th-based Fe accumulation is most closely related to Ti accumulation. While the ^{230}Th-based accumulation rates are much less well correlated than the δ^{18}O-based data and the data set is over a shorter time period, it is still clear that Fe accumulation is better correlated with opal accumulation than with the accumulation of $CaCO_3$ or TOC. If anything, the correlations between the accumulations of Fe and $CaCO_3$, as well as between Fe and TOC, are *negative*, whereas the correlation between the accumulations of Fe and opal is positive, albeit weaker than the δ^{18}O-based Fe-opal accumulation relationship (yet still with high confidence, >97%). Considering all the records, the Fe-opal relationship remains the strongest of those between Fe and any biogenic component, regardless of the method used to determine sedimentation rate.

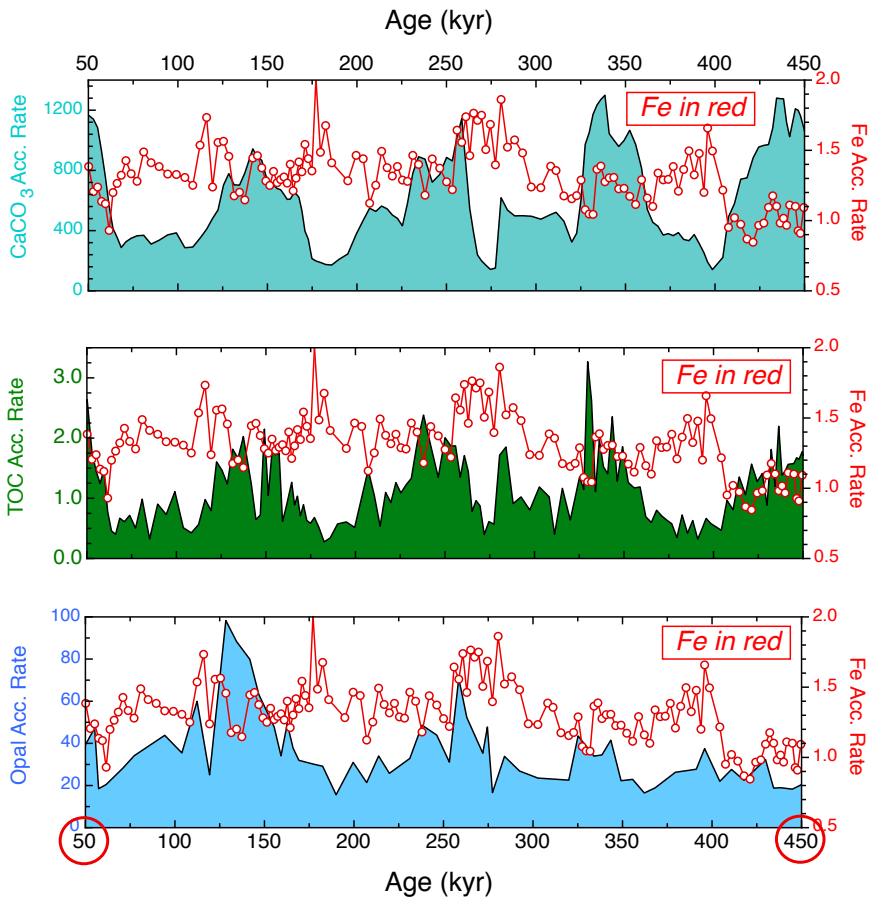

Supplementary Figure 5. Time series of the accumulation of Fe, $CaCO_3$, TOC, and opal, based on ^{230}Th-based accumulation rates (all in mg/cm^2/kyr). The record extends only from 50 kyr to 450 kyr (red circles on x-axis), due to the differences in age model for samples younger than 38 kyr and the lack of ^{230}Th data older than ~450 kyr due to U-series decay. See Supplementary Figure 6 and Supplementary Table 1 for Pearson correlation coefficients and p values.

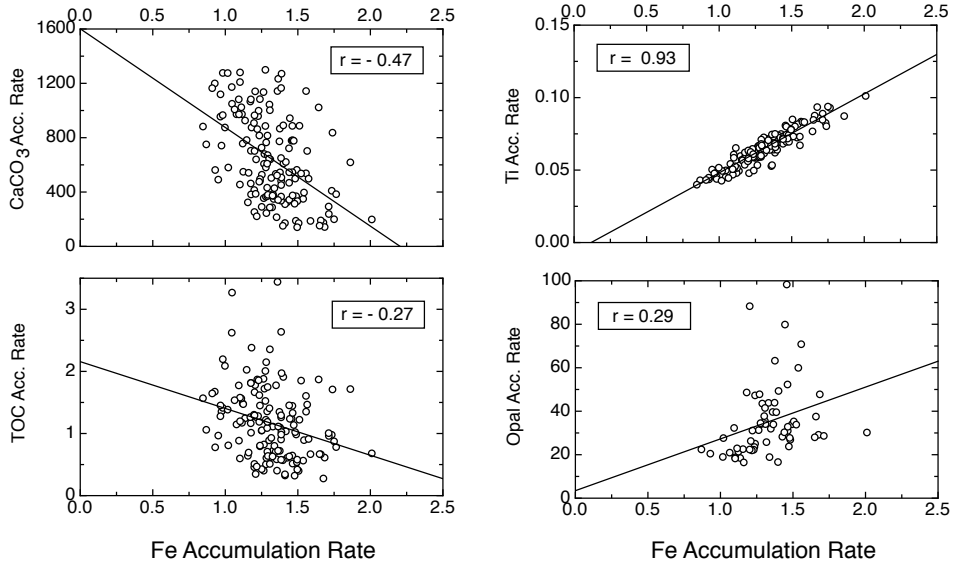

Supplementary Figure 6. Comparison of Fe-, Ti-, and biogenic accumulation rates, using the ^{230}Th-based method for sedimentation rate, with Pearson correlation coefficients (r) as shown. Units are mg/cm^2/kyr. See Supplementary Table 1 for p values.

Supplementary Table 1. Pearson correlation coefficients (r) and p values for accumulation rates between components, Core PC72, using different methods to determine sedimentation rate.

	δ^{18}O - based		^{230}Th - based	
	r	**p**	**r**	**p**
Fe - $CaCO_3$	0.16	< 0.001	- 0.47	< 0.001
Fe - Opal	0.61	< 0.001	0.29	= 0.026
Fe - TOC	0.38	< 0.001	- 0.27	= 0.001
Fe- Ti	0.97	< 0.001	0.93	< 0.001
Fe - Ba	0.95	< 0.001	0.61	< 0.001
Opal - $CaCO_3$	0.07	= 0.449	0.13	= 0.303
Opal - Ba	0.69	< 0.001	0.62	< 0.001

Fe accumulation and opal accumulation are most poorly correlated over the period from 0 kyr to 180 kyr, even with the δ^{18}O-based approach (see main text). Because the ^{230}Th-based record extends only to 450 kyr, compared to 1 Ma for the δ^{18}O-based record, the 180 kyr duration from 0 ky to 180 kyr is ~40% of the total ^{230}Th-based record. Thus, we would expect that the correlations in the ^{230}Th-based data set to be lower, independent of the true differences between the techniques. Nonetheless, the relative importance of the Fe-opal relationship is clear, as is the strong relationship between opal and Ba, and between Fe and Ba (Supplementary Table 1). On-going and future research of opal through the younger portions of the sediment[12] may shed further light on the similarities and contrasts between the younger and older records.

Core PC72 Data Sources and Methods

The oxygen isotope data ($\delta^{18}O$) and methodologies are found in ref. 4.

$CaCO_3$ data and methodologies are found in ref. 4. Concentrations were measured using standard coulometric techniques. Analytical precision is 4% of the measured value, and accuracy was checked through comparison to an independent pure $CaCO_3$ standard.

Opal data are found in Supplementary Table 2 (below). Opal was measured using the timed-dissolution technique[13]. Multiple replicate analyses of an internal standard of natural sediment from the PC72 (140W) site yielded precision of the analysis to be 0.3 weight %. Accuracy was checked against a sample analyzed at a separate laboratory.

TOC data are found in Supplementary Table 2 (below). Organic carbon was measured with a Carlo-Erba 1108 CHN elemental analyzer after removing the $CaCO_3$ component by acidification. The standard deviation of replicate analyses for PC72 was 0.02 weight percent.

Fe concentrations and methodologies are found in ref. 7 up to age 599.392 kyr. Data older than that age are presented here for the first time. Fe was measured by inductively coupled plasma emission spectrometry (ICP-ES) at Boston University. Analytical precision is 4% of the measured value, and accuracy was checked through comparison to an independent standard (NIST-1c) from the U.S. National Institute of Standards and Technology.

Ti concentrations and methodologies are found in ref. 4. Ti was measured by ICP-ES at Boston University. Analytical precision is 4% of the measured value, and accuracy was checked through comparison to an independent standard (NIST-1c) from the U.S. National Institute of Standards and Technology.

Ba concentrations and methodologies are found in ref. 4 and ref. 14. Ba was measured by ICP-ES at Boston University. Analytical precision is 4% of the measured value, and accuracy was checked by re-analyzing a suite of samples that had been previously analyzed by x-ray fluorescence during analytical runs that were constrained by independent standards.

Supplementary References

1. Murray, J. W., Barber, R. T., Roman, M. R., Bacon, M. P. & Feely, R. A. Physical and biological controls on carbon cycling in the equatorial Pacific. *Science* **266,** 58-65 (1994).

2. Barber, R. T. & Hiscock, M. R. A rising tide lifts all phytoplankton: Growth response of other phytoplankton taxa in diatom-dominated blooms. *Glob. Biogeochem. Cycles* **20,** doi:10.1029/2006GB002726 (2006).

3. Murray, R. W. & Leinen, M. Chemical transport to the seafloor of the equatorial Pacific across a latitudinal transect at 135W; Tracking sedimentary major, trace, and rare earth element fluxes at the Equator and the Intertropical Convergence Zone. *Geochim. Cosmochim. Acta* **57,** 4141-4163 (1993).

4. Murray, R. W., Knowlton, C., Leinen, M., Mix, A. C. & Polsky, C. H. Export production and carbonate dissolution in the central equatorial Pacific Ocean over the past 1 Ma. *Paleoceanography* **15,** 570-592 (2000).

5. Winckler, G., Anderson, R. F., Fleisher, M. Q., McGee, D. & Mahowald, N. Covariant glacial-interglacial dust fluxes in the equatorial Pacific and Antarctica. *Science* **320,** 93-96 (2008).

6. Anderson, R. F., Fleisher, M. Q., Lao, Y. & Winckler, G. Modern $CaCO_3$ preservation in equatorial Pacific sediments in the context of late-Pleistocene glacial cycles. *Mar. Chem.* **111,** 30-46 (2008).

7. Murray, R. W., Leinen, M., Murray, D. W., Mix, A. C. & Knowlton, C. W. Terrigenous Fe input and biogenic sedimentation in the glacial and interglacial Equatorial Pacific Ocean. *Glob. Biogeochem. Cycles* **9,** 667-684 (1995).

8. Broecker, W. Excess sediment ^{230}Th: Transport along the sea floor or enhanced water column scavenging? *Glob. Biogeochem. Cycles* **22,** doi:10.1029/2007GB003057 (2008).

9. Robinson, L. F., Noble, T. L., & McManus, J. F. Measurement of adsorbed and total ^{232}Th/^{230}Th ratios from marine sediments. *Chem. Geol.* **252,** 169-179 (2008).

10. Chase, Z., Anderson, R. F., Fleisher, M.Q. & Kubik, P. W. The influence of particle composition and particle flux on scavenging of Th, Pa and Be in the ocean. *Earth Planet. Sci. Lett.* **204,** 215-229 (2002).

11. Kretschmer, S., Geibert, W., Rutgers van der Loeff, M. M. & Mollenhauer, G. Grain size effects on $^{230}Th_{xs}$ inventories in opal-rich and carbonate-rich marine sediments. *Earth Planet. Sci. Lett.* **294,** 131-142 (2010).

12. Hayes, C., Anderson, R. F. & Fleisher, M. Q. Opal accumulation rates in the equatorial Pacific and mechanisms of deglaciation. *Paleoceanography* **26**, doi:10.1029/2010PA002008 (2011).

13. Mortlock, R.A. & Froelich, P.N. A simple method for the rapid determination of biogenic opal in pelagic marine sediments. *Deep-Sea Res.* **36,** 1415-1426 (1989).

14. Schroeder, J.O., Murray, R.W., Leinen, M., Pflaum, R.C. & Janecek, T.R. Barium in equatorial Pacific carbonate sediment: Terrigenous, oxide, and biogenic associations. *Paleoceanography* **12**, 125-146 (1997).

Supplementary Table 2. Data for Core PC72.

Dry Bulk Density calculated from $CaCO_3$ (weight %) according to ref. 3.
Linear Sedimentation Rate calculated from $\delta^{18}O$ stratigraphy from ref. 4.
$\delta^{18}O$-based Mass Accumulation Rate = (Dry Bulk Density) x ($\delta^{18}O$-based Linear Sedimentation Rate).
^{230}Th-based Mass Accumulation Rate ($mg/cm^2/kyr$), interpolated from ref. 5 and ref. 6 onto these ages.
Data for Fe from ref. 4 to 599.392 kyr.

Depth (cm)	Age [4] (1000's of yr)	$\delta^{18}O$ (ref. 4)	Dry Bulk Density (mg/cm^3)	Linear Sed. Rate (cm/kyr)	$\delta^{18}O$-based Mass Acc. Rate ($mg/cm^2/kyr$)	^{230}Th-based Mass Acc. Rate ($mg/cm^2/kyr$)	$CaCO_3$ (ref. 4) (weight %)	Opal (weight %)	TOC (weight %)	Fe (weight %)	Ti [4] (ppm)	Ba [4] (ppm)
4			742				81.5		0.21			
9			737				81.8		0.17			
14	2.738	3.39	764	1.94	1482		83.2	13.3	0.19	1514	71	1492
19	5.106	3.64	775	2.25	1741	668	83.9	13.3	0.17	1313	60	1443
24	7.203	3.44	768	2.49	1914	902	83.4	8.2	0.28	1212	55	1287
29	9.125	4.08	787	2.70	2122	951	84.8		0.11	1247	53	1236
34	10.917	4.34	787	2.87	2262	991	84.8	6.8	0.18	1144	54	1207
39	12.608	4.68	825	3.02	2492	1025	87.5		0.18	1241	62	1266
44	14.229	4.59	805	3.13	2520	1114	86.1	4.2	0.24	1247	59	1322
49	15.802	4.92	852	3.20	2729	1044	89.3		0.16	1284	51	1177
54	17.351	4.71	847	3.23	2736	1077	89.0	3.1	0.26	1380	58	1116
59	18.9	4.57	849	3.20	2715	1041	89.2		0.28	1222	57	1112
64	20.479	4.69	848	3.11	2639	999	89.1	2.8	0.09	1268	57	1031
69	22.115	4.62	846	2.97	2509	972	88.9		0.19	1403	66	1113
74	23.852	4.60	874	2.76	2411	894	90.8	1.9	0.15	1219	53	1025
79	25.744	4.59	870	2.50	2179	932	90.6		0.23	1066	47	893
84	27.86	4.48	856	2.20	1882	1122	89.6	2.8	0.25	1074	46	857
89	30.315	4.25	867	1.88	1629	993	90.3		0.15	948	45	825
94	33.219	4.36	844	1.60	1348	1203	88.8	2.9	0.13	1037	41	798
99	36.621	4.24	877	1.41	1241	1149	91.0		0.27	970	41	865
104	40.298	4.41	857	1.41	1205	1275	89.7	3.1	0.27	1067	41	800
114	47.19	4.27	870	1.57	1366	1254	90.6	2.5	0.15	1008	43	817
119	50.152	4.10	838	1.79	1503	1318	88.4	3	0.2	1050	47	901
124	52.786	4.09	858	2.00	1717	1271	89.8		0.14	948	38	731
129	55.163	4.40	857	2.18	1872	1209	89.7	3.9	0.12	1025	41	780
134	57.37	4.20	851	2.31	1965	1038	89.3	1.8	0.12	1095	48	830
139	59.494	4.31	813	2.36	1923	873	86.7		0.17	1282	55	976
144	61.599	4.41	814	2.36	1918	648	86.8	3.2	0.12	1435	67	1035
149	63.739	4.26	742	2.25	1671	509	81.5		0.09	2358	123	1722
154	66.047		716	2.17	1551	447	79.5		0.09	2832	147	2014
159	68.355	4.21	688	2.04	1405	372	77.3		0.18	3557	193	2668
164	70.963	4.23	724	1.81	1313	407	80.1	7	0.15	3508	184	2607
169	73.883	4.05	696	1.61	1124	448	77.9		0.16	2975	158	2210
174	77.179	3.73	720	1.43	1032	458	79.8	7.4	0.11	2794	140	2017
179	80.89	3.80	705	1.28	901	469	78.7		0.21	3173	167	2378
184	85.028	3.89	680	1.16	787	405	76.6		0.08	3481	182	2631
189	89.54	3.82	699	1.08	755	430	78.2		0.21	3217	164	2589
194	94.3	3.93	741	1.04	771	457	81.4	9.6	0.16	2916	152	2375
199	99.145	3.58	719	1.04	751	483	79.8		0.23	2748	146	2207
204	103.88	3.65	574	1.09	627	426	67.3	8.3	0.12	3069	147	2406
209	108.318	3.76	661	1.18	781	388	75.1		0.11	3228	159	2618
214	112.369	3.82	655	1.30	850	470	74.5	12.8	0.12	3272	154	2689
219	116.036	3.15	663	1.43	951	544	75.3		0.18	3187	152	2739
224	119.365	3.21	705	1.57	1108	611	78.7	4.1	0.13	2026	103	1958
229	122.417		607	1.64	995	765	70.3		0.21	2035	96	1766
234	125.469	3.63	681	1.66	1131	916	76.7		0.16	1708	91	1373
239	128.433	4.07	745	1.68	1252	952	81.8	10.3	0.13	1530	85	1418
244	131.421	3.93	741	1.67	1236	864	81.4		0.21	1361	71	1421
249	134.427	4.61	725	1.68	1216	876	80.2	10.1	0.19	1372	65	1333
254	137.382	4.77	790	1.74	1376	921	85.0		0.22	1246	65	1325
262	141.844	4.57	775	1.87	1446	1124	83.9	7.1	0.11	1285	65	1224
267	144.422	4.31	754	2.00	1508	1076	82.4		0.06	1358	66	1275
272	146.849	4.47	778	2.12	1651	1030	84.2	6.1	0.07	1336	62	1392
277	149.137	4.47	748	2.24	1675	934	81.9		0.23	1372	66	1254
282	151.314	4.52	767	2.35	1798	873	83.3		0.12	1433	71	1195
287	153.403	4.36	337	2.43	820	846			0.21	1596	76	1330
292	155.423	4.35	761	2.52	1916	820	82.9	5.8	0.21	1548	81	1343
297	157.375	4.45	783	2.61	2045	795	84.5		0.22	1625	80	1279
302	159.252	4.45	763	2.73	2082	771	83.1	4.4	0.08	1699	80	1308
307	161.043	4.28	738	2.86	2113	748	81.2		0.11	1692	79	1383
312	162.745	4.41	744	2.99	2228	746	81.7	6.6	0.14	1877	97	1449
317	164.384	4.49	805	3.08	2481	744	86.1		0.17	1629	83	1036
322	165.989	4.19	818	3.11	2546	742	87.0	5.1	0.12	1755	89	1302
327	167.596	4.31	776	3.07	2384	740	84.0		0.14	1916	97	1419
332	169.244	4.23	762	2.96	2260	643	83.0	5	0.11	2096	105	1581
337	170.971	4.33	614	2.79	1716	558	71.0		0.16	2762	146	1897
342	172.829	4.09	674	2.58	1740	450	76.2		0.14	3198	162	2188
347	174.854	4.29	601	2.35	1411	308	69.8		0.19	4399	234	3126
352	177.098	4.35	572	2.10	1203	296	67.0	10.2	0.23	6792	342	4770
357	179.624	3.68	561	1.86	1040	286	65.9		0.18	5194	274	3334
362	182.511	4.11	537	1.60	860	276	63.5	10.6	0.1	6077	339	4119
367	185.907	4.20	552	1.34	741	264	65.0		0.13	5349	274	3733
372	190.028	3.91	775	1.12	868	250	83.9	6.3	0.23	1725	79	1411
377	194.889	3.37	680	1.05	714	320	76.6		0.19	4013	201	2795
382	199.554	3.51	721	1.17	844	469	79.9	6.6	0.11	3119	159	2363
387	203.498	3.49	772	1.33	1027	559	83.8			2576	122	2044
392	207.091	3.56	800	1.43	1141	640	85.8	3.3	0.23	1755	80	1500
397	210.516	3.74	726	1.50	1086	657	80.3		0.16	1905	89	1500
402	213.777	3.93	771	1.25	967	673	83.7	5.1	0.08	2217	110	1833
405	216.855	3.59	780	1.68	1314	646	84.3		0.17	2131	112	1739
412	219.779	4.24	739	2.08	1540	620	81.3	4.2	0.15	2125	109	1782
417	222.603	4.33	776	1.78	1381	573	84.0		0.22	2416	122	2274
422	225.396	4.38	768	1.95	1499	518	83.4		0.21	2488	114	1907
428	228.233	4.40	734	1.73	1271	718	80.9		0.17	1781	83	1655
432	231.205	3.85	832	1.45	1206	888	88.0	3.7	0.15	1649	78	1337
437	234.427	3.82	841	1.47	1237	1006	88.6		0.19	1392	64	1018
442	238.024	4.02	835	1.31	1097	992	88.2	4.9	0.24	1190	60	900
447	242.059	3.71	647	1.22	787	978	73.8			1472	74	1038
452	246.245	4.64	726	1.25	910	963	80.3	4.6	0.14	1426	76	1071

Depth (cm)	Age [4] (1000's of yr)	$\delta^{18}O$ (ref. 4)	Dry Bulk Density (mg/cm^3)	Linear Sed. Rate (cm/kyr)	$\delta^{18}O$-based Mass Acc. Rate ($mg/cm^2/kyr$)	^{230}Th-based Mass Acc. Rate ($mg/cm^2/kyr$)	$CaCO_3$ (ref. 4) (weight %)	Opal (weight %)	TOC (weight %)	Fe (weight %)	Ti [4] (ppm)	Ba [4] (ppm)
457	250.055	4.44	837	1.43	1197	1003	88.3		0.2	1272	67	1034
462	253.286	4.42	828	1.73	1429	984	87.7	3.2	0.19	1240	61	978
467	255.912		825	1.90	1571	1169	87.5		0.16	1406	66	960
472	258.539	4.59	784	2.04	1601	1352	84.6	5.2	0.1	1152	50	1026
477	260.831	4.47	701	2.23	1566	1068	78.3		0.16	1628	75	1063
482	263.02	4.50	714	2.30	1641	688	79.3	7.6	0.21	2125	116	1498
487	265.183		646	2.31	1493	521	73.8		0.15	3387	178	2228
492	267.345	4.59	571	2.27	1296	356	66.9		0.27	4811	250	3243
497	269.59	4.43	542	2.17	1175	312	64.0		0.28	5607	301	3699
502	271.959	4.25	547	2.03	1109	265	64.5	13.3	0.15	5670	320	3587
507	274.527	4.48	489	1.86	908	245	58.2	19.5	0.25	6878	350	4717
512	277.352	4.15	621	1.67	1040	211	71.6	7.9	0.27	6614	323	4062
517	280.517	3.94	919	1.49	1372	660	93.8		0.26	2822	132	1779
522	284.077	3.69	817	1.33	1085	617	86.9	5.5	0.3	2466	130	1757
527	288.069	4.11	824	1.19	982	570	87.4		0.16	2762	146	1969
532	292.488	4.34	830	1.08	896	568	87.8	4.7	0.18	2608	122	1833
537	297.356	4.16	806	0.98	790	575	86.2		0.14	2154	102	1676
542	302.712	4.00	778	0.92	717	566	84.2	4.2	0.21	2181	105	1720
547	308.207	3.90	848	0.96	811	569	89.1		0.18	2438	118	1889
550	311.199	3.83	874	1.30	1135	575	90.8		0.07	2360	116	1756
557	315.591		944	1.48	1398	486	95.3		0.24	2421	120	1851
563	319.982	3.48	734	1.42	1039	401	80.9	5.6	0.16	2884	142	2285
567	322.712	3.32	815	1.95	1587	440	86.8		0.23	2674	141	2364
573	325.185	3.35	794	2.08	1652	714	85.3	6.1	0.19	1806	84	1603
577	327.493	3.31	913	2.22	2028	1042	93.3		0.11	1034	52	1041
583	329.706	3.30	860	2.28	1961	1167	89.9		0.28	896	43	949
587	331.873	3.85	853	2.30	1960	1312	89.4		0.2	796	34	1042
593	334.056		842	2.29	1929	1391	88.7	2.4	0.08	981	38	881
597	336.239	3.70	866	2.23	1933	1408	90.3		0.14	985	47	746
603	338.516	3.84	919	2.36	2172	1386	93.8	2.5	0.11	921	47	708
608	340.908	3.93	848	2.02	1716	1172	89.1		0.12	1113	55	951
613	343.464	4.60	852	1.71	1453	1122	89.4	3.7	0.21	1165	65	946
617	346.215	4.41	859	1.74	1492	1067	89.8		0.12	1149	60	1006
623	349.188	4.49	883	1.64	1447	1092	91.4	2	0.17	1126	59	864
627	352.363	4.44	905	1.54	1393	1149	92.8		0.11	1021	49	799
633	355.661	4.25	882	1.51	1336	1066	91.3	2.2	0.11	1046	61	796
637	358.966	4.19	851	1.54	1310	914	89.3		0.13	1412	78	985
643	362.176	4.20	802	1.59	1272	630	85.9	2.6	0.11	1841	90	1283
647	365.249	4.30	771	1.67	1287	544	83.7		0.11	2023	112	1354
653	368.194	4.25	797	1.72	1370	501	85.5	3.8	0.16	2671	141	1650
657	371.048	4.15	703	1.77	1244	472	78.5		0.15	2733	144	1826
663	373.859	3.82	767	1.78	1362	456	83.3		0.14	2837	147	1728
667	376.678	4.18	757	1.76	1328	444	82.6		0.13	3118	155	1802
673	379.546	4.19	847	1.73	1463	435	89.0	6.1	0.08	2782	142	1692
677	382.481	3.99	726	1.69	1226	426	80.3		0.17	3204	175	2025
683	385.457	3.92	714	1.69	1206	420	79.3		0.1	3563	186	2305
687	388.394	3.94	762	1.75	1334	451	83.0		0.14	2942	141	1947
693	391.2	3.95	699	1.83	1280	402	78.2	6.9	0.08	3678	184	2344
697	393.824	3.73	653	1.74	1138	340	74.3		0.15	3529	187	2518
701	395.86	3.98	562	2.09	1176	289	66.0	13	0.23	5733	303	4037
707	398.559	3.59	535	1.89	1010	223	63.3		0.26	6710	349	4851
716	404.349	3.44	668	1.56	1045	293	75.7	7.5	0.16	4156	214	2968
721	407.528	3.62	809	1.53	1239	569	86.4		0.17	1673	89	1601
726	410.886	2.96	805	1.46	1177	674	86.1	4.1	0.12	1513	73	1457
731	414.367	3.40	827	1.43	1185	846	87.7		0.16	1151	57	1126
736	417.867	3.52	790	1.45	1148	883	85.0	2.5	0.12	984	49	965
741	421.245	3.85	862	1.53	1322	980	90.0		0.16	863	41	807
746	424.396	4.14	857	1.66	1426	1065	89.7		0.12	907	43	762
751	427.266	4.27	846	1.83	1544	1087	88.9		0.13	904	42	768
756	429.883	4.42	830	2.01	1671	1106	87.8	2.9	0.08	989	42	769
761	432.246	4.29	856	2.22	1896	1208	89.6		0.15	974	44	730
766	434.405	4.77	959	2.41	2310	1330	96.3	1.4	0.09	828	38	717
771	436.404	4.88	908	2.59	2352	1373	93.0		0.16	716	32	657
776	438.268	4.86	895	2.80	2506	1384	92.2	1.4	0.1	734	31	643
781	439.979		900	2.92	2629	1210	92.5		0.12	799	39	729
786	441.691	4.94	887	3.03	2685	1117	91.7		0.14	994	47	774
796	444.882	4.45	892	3.17	2830	1314	92.0	1.4	0.12	838	45	820
801	446.439	4.74	910	3.20	2911	1288	93.2		0.13	720	35	632
805	447.695		892	3.19	2842	1266	92.0		0.13	719	34	640
811	449.578	4.61	884	3.14	2774	1183	91.5		0.15	924	43	721
816	451.198	4.47	891	3.03	2698	1097	91.9	1.9	0.14	970	41	812
821	452.88	4.46	872	2.90	2528	1002	90.7		0.13	1196	56	903
826	454.648	4.42	874	2.75	2408	898	90.8		0.18	1374	68	1024
831	456.514	4.42	895	2.61	2331	949	92.2		0.22	1051	54	874
836	458.488	4.53	857	2.47	2118	1076	89.7	2.1	0.12	1116	54	827
841	460.561	4.31	820	2.37	1947	1018	87.2		0.12	1484	72	1108
846	462.702	4.30	846	2.32	1961	874	88.9	2.7	0.13	1683	82	1201
851	464.874	4.28	797	2.30	1835	761	85.5		0.17	1820	90	1172
856	467.044	4.26	757	2.31	1747	660	82.6	4.6	0.22	2181	108	1451
861	469.204	4.27	758	2.31	1754	546	82.7		0.18	2536	137	1731
866	471.364	4.15	636	2.30	1463	402	72.9	7.1	0.25	4256	211	2886
871	473.552	4.18	547	2.25	1232	290	64.5		0.23	5467	286	3659
876	475.802	3.90	520	2.17	1128	248	61.7	11.3	0.27	6663	342	4540
881	478.16	3.84	568	2.05	1165		66.7		0.26	5426	272	3196
886	480.685	4.03	684	1.42	968		76.9		0.18	4860	215	2873
891	486.557	3.75	783	1.82	1426		84.5		0.22	2232	114	1476
896	488.347		863	2.79	2411		90.1	4.2	0.17	1879	92	1302
901	490.137	3.38	723	1.99	1437		80.0		0.24	1547	69	1139
906	494.36	3.90	788	1.10	865		84.9		0.12	1477	68	981
911	499.311	3.43	842	1.00	840		88.7		0.08	1645	82	1143
916	504.386		830	0.99	818		87.9	3.2	0.2	1724	80	1114
921	509.461	4.09	832	1.16	968		88.0		0.17	1629	73	1068
926	513.191	4.02	820	1.52	1249		87.2		0.15	1479	69	1135
931	516.125	4.17	884	1.87	1655		91.5		0.12	1394	60	990
936	518.577	3.75	852	2.16	1842		89.3	3.5	0.12	1195	52	889

Depth (cm)	Age [4] (1000's of yr)	$\delta^{18}O$ (ref. 4)	Dry Bulk Density (mg/cm^3)	Linear Sed. Rate (cm/kyr)	$\delta^{18}O$-based Mass Acc. Rate ($mg/cm^2/kyr$)	^{230}Th-based Mass Acc. Rate ($mg/cm^2/kyr$)	$CaCO_3$ (ref. 4) (weight %)	Opal (weight %)	TOC (weight %)	Fe (weight %)	Ti [4] (ppm)	Ba [4] (ppm)
941	520.764	3.80	874	2.36	2066		90.8		0.15	1050	45	812
946	522.813	3.60	882	2.44	2155		91.3	2	0.14	937	44	694
951	524.857		900	2.45	2201		92.5		0.12	890	39	641
956	526.901	3.83	905	2.33	2108		92.8	2.1	0.12	905	41	729
961	529.161	4.18	931	2.05	1911		94.5		0.12	1025	43	733
966	531.803	3.84	881	1.67	1472		91.3		0.13	1193	49	984
971	535.253	4.06	914	1.18	1079		93.4		0.11	1292	56	1030
976	540.738	4.15	920	0.71	655		93.8		0.15	1004	46	788
981	550.518	4.11	922	0.55	507		93.9		0.16	1045	46	820
986	558.998	4.00	854	0.58	496		89.5	2.9	0.23	1358	61	1081
991	567.759	4.08	881	1.70	1501		91.3		0.15	1656	79	1385
996	569.521		847	2.84	2404		89.0	2.4	0.14	1892	92	1449
1001	571.282		836	2.84	2373		88.3		0.24	1951	96	1488
1007	573.396	3.73	841	2.62	2207		88.6	2.5	0.17	2481	93	1411
1012	575.47	3.58	760	2.50	1898		82.8		0.07	2053	103	1640
1017	577.404	3.69	780	2.63	2056		84.3	4	0.19	3156	106	1766
1022	579.267	3.34	832	2.70	2243		88.0		0.15	1993	85	1498
1027	581.114	3.35	830	2.68	2227		87.8	2.6	0.14	1659	61	1302
1032	582.993	3.56	857	2.61	2232		89.7		0.15	1304	46	1018
1037	584.954	3.61	879	2.47	2176		91.2	1.9	0.16	1254	60	1062
1042	587.038	4.03	897	2.32	2078		92.3		0.14	817	49	1027
1047	589.278	3.46	856	2.16	1848		89.6		0.06	1079	51	1234
1052	591.672	3.78	851	2.04	1734		89.3		0.15	1225	55	1357
1057	594.186	3.67	843	1.96	1655		88.8	3.1	0.1	1432	71	1521
1062	596.769	3.47	838	1.92	1610		88.4		0.09	1478	66	1387
1067	599.392	3.97	873	1.89	1647		90.8		0.14	1299	64	1337
1072	602.071	3.68	863	1.83	1576		90.1		0.07	1336	57	1302
1077	604.871	3.51	826	1.72	1422		87.6	3.2	0.15	1445	71	1453
1082	607.888	3.45	823	1.57	1292		87.3			1418	61	1445
1087	611.256	3.36	852	1.39	1181		89.3	3.1		1134	48	1202
1092	615.136	3.64	860	1.19	1026		89.9			1060	50	1061
1097	619.696	3.70	835	1.02	854		88.2	2.7	0.09	947	44	729
1102	624.963	4.64	868	0.92	795		90.4		0.14	1229	51	917
1107	630.624	4.76	859	0.90	775		89.8		0.1	1079	37	810
1112	636.057	4.49	915	0.98	899		93.5		0.14	1108	42	897
1117	640.845	4.77	895	1.12	1003		92.2	1.4	0.09	891	41	806
1122	645.015	4.48	893	1.28	1139		92.1			1109	38	797
1127	648.716	4.55	900	1.45	1308		92.5	0.9	0.1	1120	35	614
1137	655.137	4.63	920	1.67	1541		93.8	0.8	0.05	697	34	569
1142	657.928	4.48	934	1.88	1757		94.7		0.06	806	32	543
1147	660.464	4.43	901	1.85	1663		92.6	3.9	0.11	577	23	462
1151	662.789	4.41	931	2.18	2033		94.5		0.25	872	27	559
1156	664.678		919	2.65	2434		93.8	1.1	0.15	642	29	575
1161	666.566	4.52	888	2.61	2314		91.8		0.15	1636	28	658
1166	668.517	4.38	915	2.60	2379		93.5	1.1	0.19	977	40	738
1171	670.412	4.24	911	2.65	2418		93.3		0.21	833	34	761
1176	672.286	4.14	926	2.63	2440		94.2	2.2	0.08	992	52	1025
1186	676.132		754	2.57	1942		82.4	1.8	0.17	1137	67	1128
1191	678.094	4.25	887	2.46	2183		91.7		0.17	1320	56	1205
1196	680.199	4.39	854	2.30	1966		89.5	1.9	0.12	748	62	1162
1201	682.444	4.26	804	2.15	1724		86.0		0.08	2056	105	1944
1206	684.866	3.57	804	1.97	1587		86.0		0.07	1802	92	1843
1211	687.518	3.33	846	1.75	1484		88.9		0.07	1538	73	1432
1216	690.597		859	1.62	1395		89.8	2.1	0.09	936	37	854
1221	693.677	3.70	862	1.48	1279		90.0		0.11	808	37	786
1226	697.393		868	1.35	1168		90.4	2.5	0.22	719	27	636
1231	701.109	3.97	837	1.28	1075		88.3		0.26	648	26	607
1236	705.198		852	1.22	1042		89.3	1.7	0.09	575	27	615
1241	709.287	3.90	884	1.25	1105		91.5		0.1	590	24	587
1246	713.205	4.24	893	1.33	1187		92.1		0.07	671	36	650
1251	716.822	4.54	905	1.44	1304		92.8		0.16	932	41	655
1256	720.155	4.46	906	1.54	1399		92.9	2.1	0.13	1345	53	1013
1261	723.303	4.41	913	1.60	1459		93.3		0.21	1074	46	867
1266	726.409	4.21	925	1.58	1460		94.1		0.17	898		760
1271	729.641	4.13	964	1.47	1419		96.5		0.19	817	31	659
1276	733.217	3.95	905	1.22	1108		92.8	1.5	0.06	521	18	419
1281	737.98		923	1.05	969		94.0		0.24	722	35	630
1286	742.743	4.05	928	0.92	854		94.3	1.1	0.13	672	25	552
1291	749.075	4.25	911	0.80	727		93.3		0.14	799	20	479
1296	755.289	4.08	918	0.89	815		93.7	1.7	0.21	545	29	579
1301	760.433	4.11	888	1.22	1080		91.8		0.07	567	22	467
1306	763.858		858	1.46	1253		89.8	2.6	0.16	717	44	606
1311	767.284		932	1.46	1361		94.6		0.17	1062	69	835
1316	770.709	4.04	911	1.75	1599		93.3		0.09	1356	71	957
1321	773.149	4.09	805	2.17	1750		86.1		0.16	1517	79	1052
1326	775.323	3.79	824	2.40	1980		87.4	3.3	0.15	2006	120	1567
1331	777.318	4.14	752	2.59	1944		82.3		0.18	2324	124	1893
1336	779.195	3.50	766	2.72	2079		83.3		0.11	2699	161	2294
1341	781.002	3.14	823	2.79	2297		87.3		0.21	2201	110	1668
1346	782.776	3.48	910	3.17	2886		93.2	1.2	0.06	972	49	858
1351	784.195	3.26	917	2.92	2674		93.6		0.16	726	39	754
1356	786.358	3.72	858	2.49	2140		89.8	1.5	0.17	581	28	502
1361	788.226	4.39	881	2.61	2296		91.3		0.09	719	32	560
1366	790.196	4.38	869	2.44	2124		90.5	2.1	0.11	763	38	711
1371	792.324	4.01	859	2.23	1916		89.8		0.15	1151	60	877
1376	794.694	4.06	869	1.96	1704		90.5		0.1	1316		935
1381	797.455	4.38	882	1.64	1444		91.3		0.06	1379	65	962
1386	800.868	4.37	859	1.27	1095		89.8	1.9	0.14	1187	72	888
1391	805.477	4.22	857	0.92	790		89.7		0.09	1346	77	1001
1396	812.065	3.76	868	0.77	665		90.4		0.11	1615	83	1306
1401	818.532	3.81	847	0.72	609		89.0		0.07	1515	78	1140
1406	826.045	3.78	808	0.74	598		86.3		0.11	1906	111	1328
1411	832.193	3.22	805	0.89	720		86.1		0.12	2113	111	1534
1416	837.321		720	0.98	702		79.8	6.2	0.21	3195	177	2552
1421	842.449	3.70	764	0.97	739		83.2		0.23	2242	127	1799

Depth (cm)	Age [4] (1000's of yr)	$\delta^{18}O$ (ref. 4)	Dry Bulk Density (mg/cm^3)	Linear Sed. Rate (cm/kyr)	$\delta^{18}O$-based Mass Acc. Rate ($mg/cm^2/kyr$)	^{230}Th-based Mass Acc. Rate ($mg/cm^2/kyr$)	$CaCO_3$ (ref. 4) (weight %)	Opal (weight %)	TOC (weight %)	Fe (weight %)	Ti [4] (ppm)	Ba [4] (ppm)
1426	847.666	3.60	692	0.88	611		77.6	10.7	0.23	2726	141	2036
1431	853.857	3.60	798	0.75	600		85.6		0.12	1629	74	1359
1436	861.044	3.65	818	0.75	615		87.0	3.1	0.06	1439	62	1096
1441	867.232	4.09	819	0.88	724		87.1		0.17	1959	68	950
1446	872.446	4.38	843	0.97	822		88.8		0.07	1356	69	1160
1451	877.495	4.47	840	0.95	799		88.5		0.12	1253	61	1247
1456	882.968	4.45	858	0.85	727		89.8		0.18	1214	66	1001
1461	889.367	4.38	869	0.72	628		90.5		0.13	1123	74	1081
1466	896.906	4.25	829	0.64	527		87.8		0.19	1598	89	1185
1471	905.137	3.93	863	0.63	544		90.1		0.21	1514	77	1283
1476	912.781	4.20	869	0.76	657		90.5		0.16	850	53	769
1481	918.605	4.00	913	1.01	919		93.4		0.14	886	53	790
1486	922.938	3.88	909	1.38	1258		93.1	1.9	0.15	767	119	673
1491	926.035		854	1.61	1379		89.5		0.06	967	50	758
1496	929.133		849	1.61	1371		89.2	2.6	0.19	1250	67	969
1501	932.231		867	1.61	1399		90.3		0.19	1440	66	999
1506	935.328	3.74	763	1.75	1335		83.1		0.17	2324	136	1447
1511	937.981		655	1.88	1234		74.5		0.19	3391	180	2726
1516	940.634	3.70	702	1.81	1268		78.4		0.17	2076	121	2018
1521	943.531	3.52	788	1.63	1288		84.9		0.21	2262	122	2110
1526	946.772	3.30	823	1.36	1116		87.3		0.26	1654	83	1528
1531	951.043		847	1.17	992		89.0		0.06	1204	60	1289
1536	955.313	3.32	844	0.99	840		88.8		0.25	1177	54	1133
1541	961.424	4.00	821	0.82	675		87.3		0.22	1538	78	1109
1546	967.486	4.18	793	0.65	516		85.3	4	0.08	2252	110	1750
1551	977.991	3.89	821	0.51	422		87.3		0.07	2520	122	2019
1556	987.049	3.60	856	0.56	478		89.6	3	0.12	1254	57	1232
1561	995.896	3.75	857	0.56	484		89.7		0.07	768	32	735
1566	1004.765	4.01	908	0.57	514		93.0	1.4	0.12	1498	76	1210
1571	1013.561	3.96	886	0.60	530		91.6		0.09	1309	69	1201
1576	1021.505	3.43	902	0.75	676		92.7		0.08	836	44	753
1582	1028.413	3.84	896	0.74	665		92.3		0.11	1018	49	753
1586	1034.904	3.93	680	0.79	537		76.6	1.2	0.07	889	38	639
1591	1040.087	4.01	874	0.77	675		90.8		0.18	1479	73	873
1594	1045.269	3.90	825	1.05	868		87.5	3.3	0.15	2089	106	1094